



Flavour Physics at FCC-ee with focus on $B_c \rightarrow \tau \nu$ ($\tau \rightarrow 3\pi \nu$)

EPS-HEP conference 2021

July 26, 2021
Clement Helsens, CERN-EP

Flavour Physics at FCC-ee: Brief Overview



- Strong case for flavour physics at the Z^0 -pole at FCC-ee
- Production of up to 5×10^{12} Z^0 's anticipated with 4 IPs
 - 7.6×10^{11} bb
 - 6.1×10^{11} cc
 - 1.7×10^{11} $\tau\tau$
- Z^0 production rate of ~ 100 kHz and clean e^+e^- environment allows triggerless readout
 - No efficiency losses from online selection cuts
- We must identify the physics cases where FCC-ee can perform better than either LHCb Upgrade II or Belle II

Species Yields at FCC-ee (per IP per year)



- Production fractions from $e^+e^- \rightarrow Z^0 \rightarrow ff$
- No efficiency factors from reconstruction or selection included

Z^0 mode	Species	Production fraction	Yield
bb	B^\pm	0.43	4.9×10^{10}
bb	B^0	0.43	4.9×10^{10}
bb	B_s^0	0.098	1.1×10^{10}
bb	B_c^\pm	4×10^{-4}	4.5×10^7
$\tau\tau$	τ	1	2.5×10^{10}
cc	D^\pm	0.43	3.9×10^{10}

Examples: Fully rec. modes with charged tracks



- $B^0 \rightarrow (K^{*0} \rightarrow K\pi) e^+ e^-$
 - Rare decay involving $b \rightarrow s$ transition ($B = 3.4 \times 10^{-7}$), sensitive to NP in loop-level processes
 - Measurement of electron mode challenging at LHCb - Expect $\sim 140k$ events with 4 IPs
- $B^0 \rightarrow \mu^+ \mu^-$
 - Very rare decay (in SM $B = 1.07 \times 10^{-10}$) which is sensitive to NP contributions
 - Well motivated for observation and $< 10\%$ B precision - Expect ~ 80 events with 4 IPs
- $B_s^0 \rightarrow (D_s^- \rightarrow K^+ K^- \pi^-) K^+$
 - Time dependent CP violation due to interference between mix. and dec. amplitudes
 - Interesting for FCC-ee because Belle-II does not resolve B_s^0 time-dependence, LHCb flavour tagging is poor - Expect ~ 2 millions events with 4 IPs

$B_c \rightarrow \tau \nu$ ($\tau \rightarrow 3\pi \nu$) prospects at FCC-ee

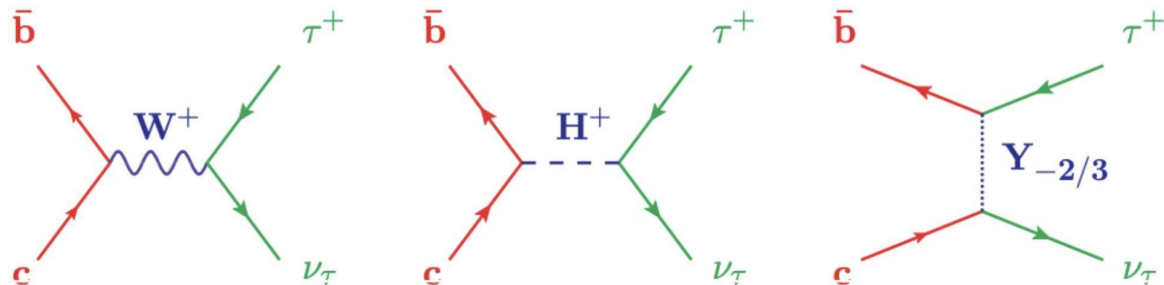


<https://arxiv.org/abs/2105.13330>

Being submitted to JHEP

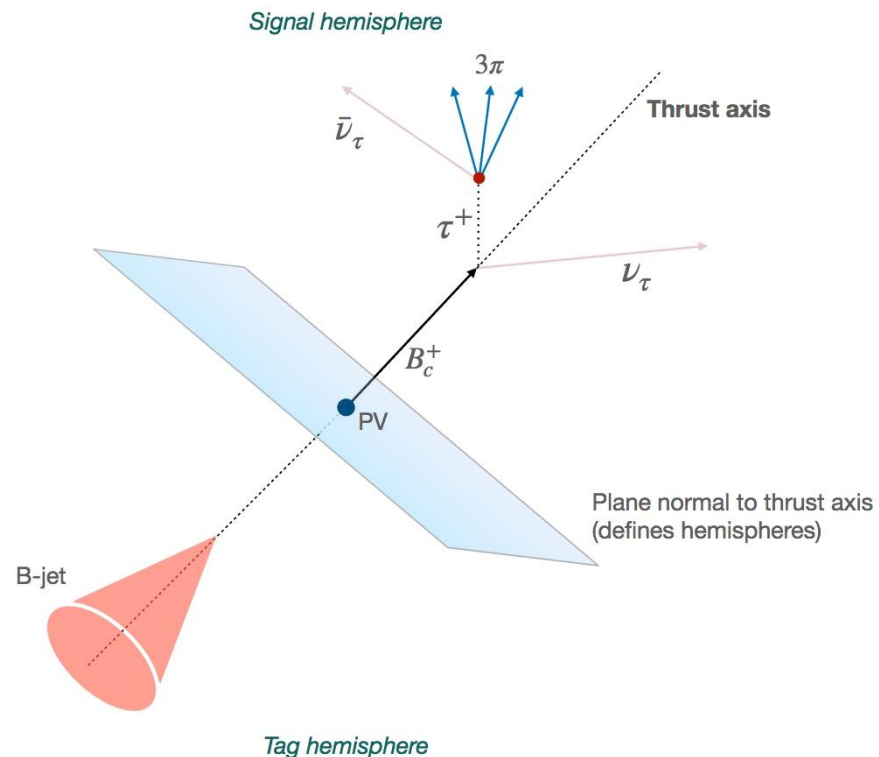
Motivation

- $B_c \rightarrow \tau \nu_\tau$ is a unique flavour opportunity at FCC-ee
 - Not possible at LHCb due to missing energy, lack of constraints and reconstructed info.
 - No B_c mesons produced at Belle II
- Involves the same Feynman vertex factors as $b \rightarrow c \tau \nu_\tau$ decays
 - Measurements of $R(D)$ and $R(D^*)$ show a $\sim 3\text{-}4\sigma$ tension with the Standard Model
 - Measuring $B(B_c \rightarrow \tau \nu_\tau)$ would provide an independent test of lepton universality and yield strong constraints on possible new physics explanations
 - $B(B_c \rightarrow \tau \nu_\tau)$ SM = $(1.94 \pm 0.09) \%$



Event topology for $B_c \rightarrow \tau \nu_\tau$

- The reconstruction of the thrust axis is used to define in which hemisphere the particles fall in
- Due to large missing energy, 2 neutrinos in the signal decay, the 2 hemisphere have rather different energy distributions



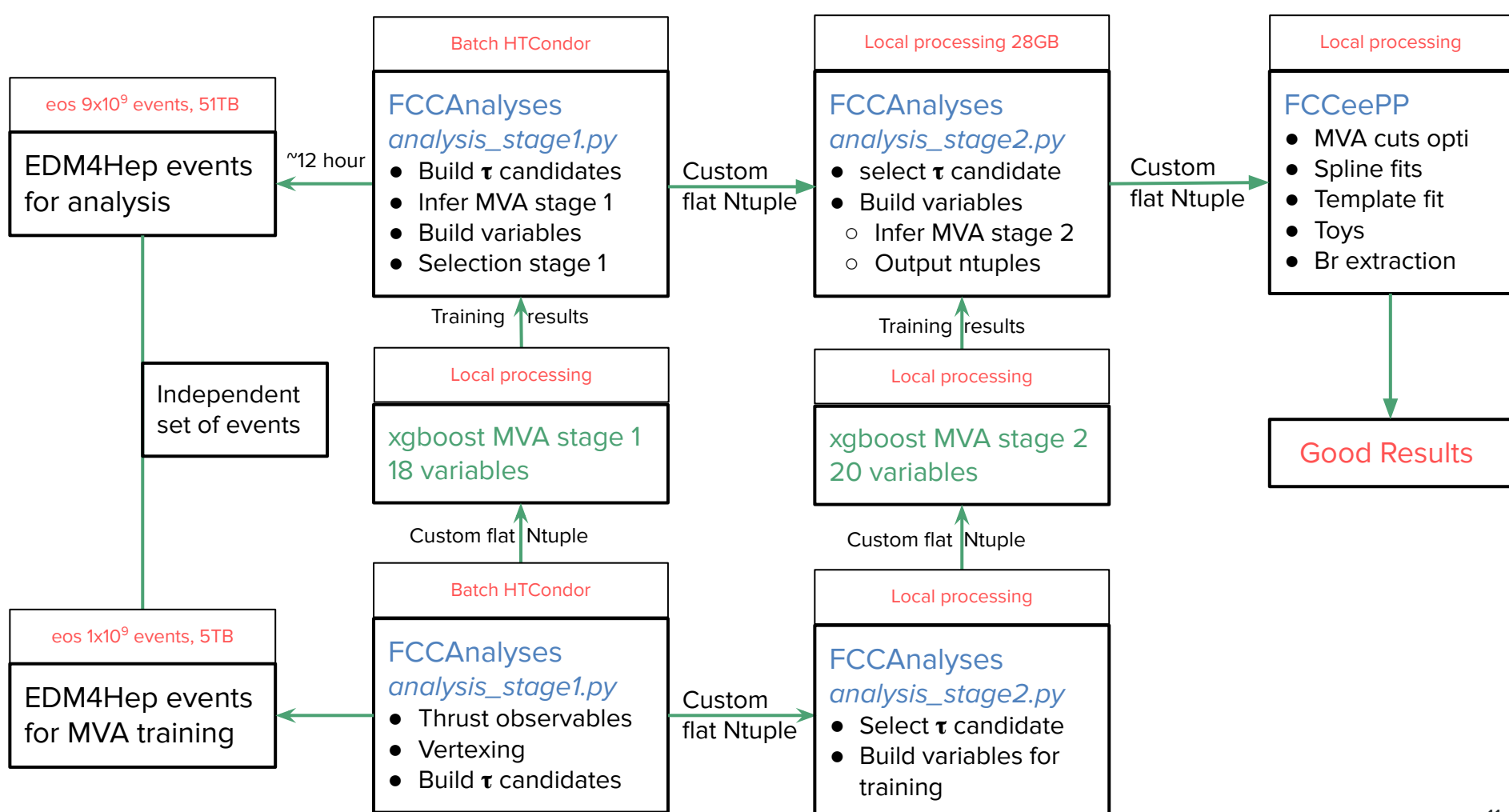
Using $\tau^- \rightarrow \pi^+ \pi^- \pi^- \nu_\tau$

- Existing feasibility study for CEPC (arxiv:2007.08234)
 - Using leptonic electron and muon tau decays
- Using tree-prong hadronic mode for this work
 - Provides τ decay vertex, and thus a measure of combined Bc and τ flight
 - Branching fraction of 9% provides sufficient decay rate
- Reject background from $Z \rightarrow bb/cc/qq$ using
 - Event level energy properties
 - Properties of the reconstructed 3π candidate
 - Two stage MVA approach

Samples and Software

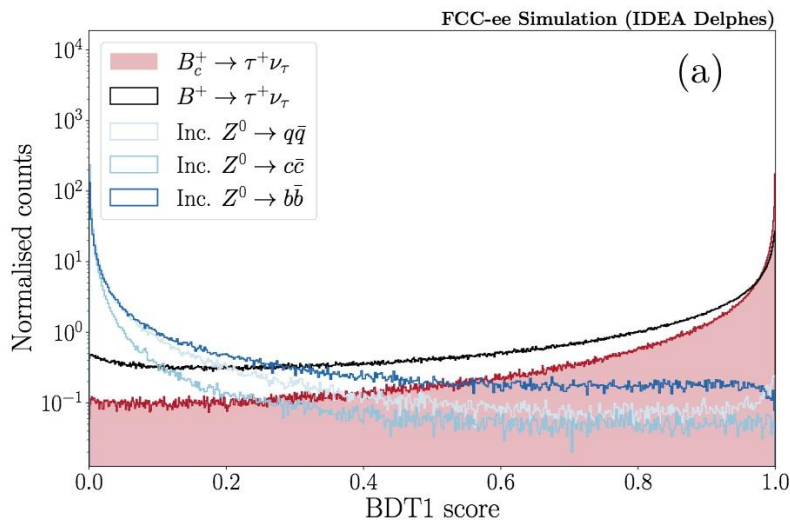


- Using official FCC-ee production ([see here](#))
 - 10^6 signal events with $\tau^- \rightarrow \pi^+ \pi^- \pi^- \nu_\tau$ generated with EvtGen
 - 10^9 events Zbb/cc/qq with Pythia8
 - Samples of exclusive B hadron background decays generated to study selection efficiency more accurately 200×10^6 per decay times 28 species
 - Dedicated orthogonal production of 10^9 events for MVA training ([see here](#))
- First published result using common software
 - Events generated with [key4Hep](#) software stack in the [EDM4Hep](#) data format
 - EDM4Hep events processed with [FCCAnalyses](#) to produce “flat ntuples”
 - Set of [custom Python analysis tools](#) to process the “flat ntuples” and produce results



First stage MVA

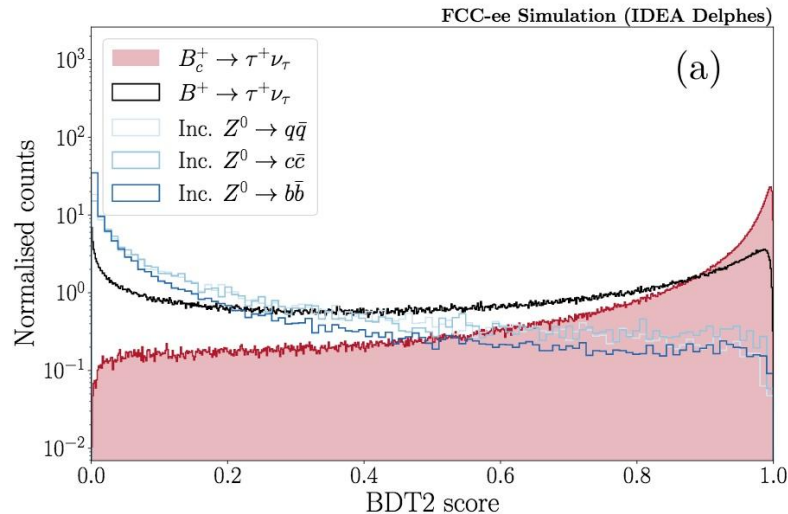
- Cuts applied before training
 - A primary vertex
 - ≥ 1 reconstructed 3π candidate
 - 1 of the 3π must be in lower E hemis.



- Train on
 - general event-level properties, harnessing difference in hemis. energies between Bc and $Z \rightarrow b\bar{b}/c\bar{c}/q\bar{q}$
 - Information on PV multiplicity, number of vertices, number of 3π cand, distance between decay vtx and PV
- Strong rejection of all three BG
 - ROC = 0.984
 - $Z \rightarrow b\bar{b}$ rejected less (produces EMiss)
 - Expect 5 times more B^+ than Bc

Second stage MVA

- Cuts applied before training
 - $MVA1 > 0.6$ (remove easy stuff)
 - 3π cand with smallest χ^2 in less E hemis
 - $m(\pi\pi)$ cuts to 3π cand $[0.6, 1]$ GeV ($\tau \rightarrow a1 \rightarrow \rho\pi$)
 - $m(3\pi) < m_\tau$, E diff in hemis > 10 GeV



- Train on
 - Properties of the 3π cand (mass momentum, IP, distance from PV, angle of momentum to thrust axis)
 - Use IP to the PV for other decay vertices
 - Mass of PV, nominal B energy
- Strong rejection of all three BG
 - ROC = 0.966
 - Excellent rejection of B^+ even if not used in the training, this reduces it to a level where it should be constraint from external measurement

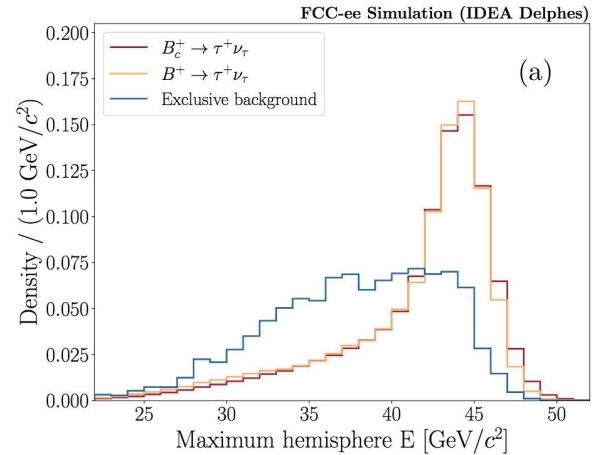
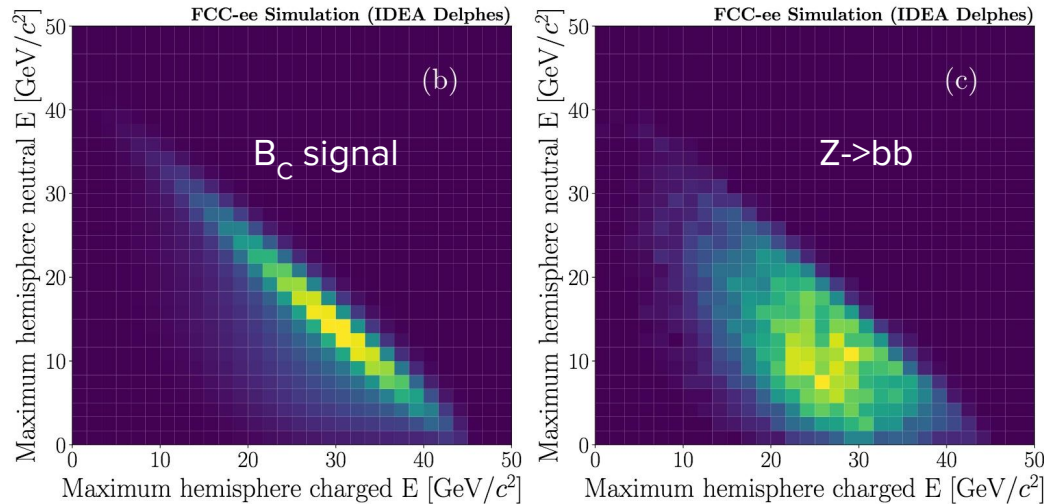
MVA cuts optimisation

- Tune the two MVA cuts to maximise purity $S/(S+B)$
 - Estimate S and B expected from 5×10^{12} Z
- Inclusive $Z \rightarrow cc/qq$ rejected at 10^9 level with sufficiently tight MVA cuts
 - Do not consider these in subsequent studies
- Estimated yields
 - With $B(Z \rightarrow bb) = 0.1512$, $B(Bc^+ \rightarrow \tau^+ \nu_\tau) = 1.94\%$ (SM pred), $f_c = 0.0004$ from Pythia and selection efficiency from signal MC
 - $B(B^+ \rightarrow \tau^+ \nu_\tau)$ using PDG B's production fractions and MC
 - Best signal yields of 4295 events with 85% purity ($\epsilon = 0.39\%$)
 - 285 events expected for B^+ ($\epsilon = 4.3 \times 10^{-5}$)
 - Background level of 448 events estimated from sum of all exclusive modes, scaled by 2.5 (inclusive vs. exclusive ratio)

Signal vs. background discrimination for fit

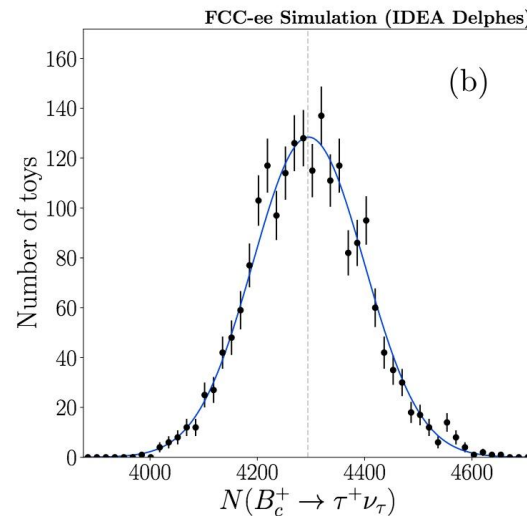
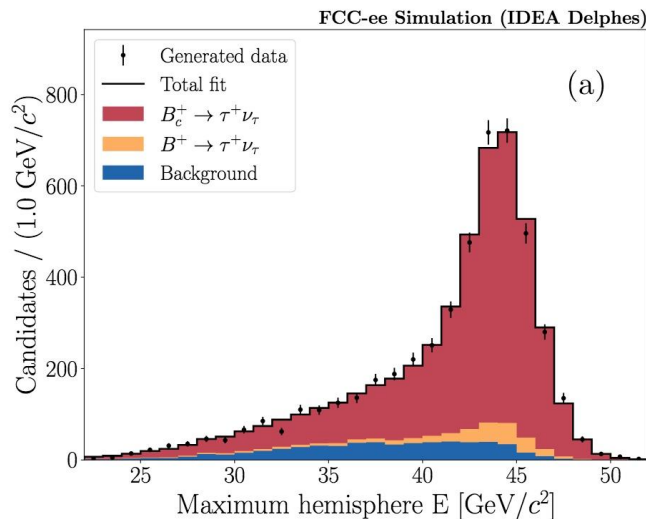


- In an inclusive Zbb event, either side could have max. E
 - However, in a signal decay, the max. E hemis is most likely the non-signal side
 - In signal events, max. E hemisphere looks a lot like an inclusive decay peak near $m(Z)/2$
 - In BG, the selection req. bias this hemisphere down in energy, giving discrimination



Toy Fit to Measure Signal Yield

- Toy dataset generated from signal and background PDFs
 - Each bin is Poisson varied independently to create toys
- Signal and background yields vary freely in the toy fit
 - signal measured with 2.4% precision
 - Fit with 10x higher background



Convert Signal Yields to $\mathcal{B}(B_c \rightarrow \tau \nu_\tau)$

$$\begin{aligned}
 R_c &= \frac{\mathcal{B}(B_c^+ \rightarrow \tau^+ \nu_\tau)}{\mathcal{B}(B_c^+ \rightarrow J/\psi \mu^+ \nu_\mu)} \\
 &= \frac{N(B_c^+ \rightarrow \tau^+ \nu_\tau)}{N(B_c^+ \rightarrow J/\psi \mu^+ \nu_\mu)} \times \frac{\epsilon(B_c^+ \rightarrow J/\psi \mu^+ \nu_\mu)}{\epsilon(B_c^+ \rightarrow \tau^+ \nu_\tau)} \times \frac{\mathcal{B}(J/\psi \rightarrow \mu^+ \mu^-)}{\mathcal{B}(\tau^+ \rightarrow \pi^+ \pi^+ \pi^- \bar{\nu}_\tau)}
 \end{aligned}$$

$$\mathcal{B}(B_c^+ \rightarrow \tau^+ \nu_\tau) = R_c \times \mathcal{B}(B_c^+ \rightarrow J/\psi \mu^+ \nu_\mu)^{\text{SM}}$$

Term	Value	Explanation
$\epsilon(B_c^+ \rightarrow \tau^+ \nu_\tau)$	$(3.93 \pm 0.04) \times 10^{-3}$	From our MC (assume 1% precision)
$\epsilon(B_c^+ \rightarrow J/\psi \mu^+ \nu_\mu)$	0.100 ± 0.001	Assume with 1% precision
$\mathcal{B}(J/\psi \rightarrow \mu\mu)$	$(5.96 \pm 0.03) \times 10^{-2}$	From PDG
$\mathcal{B}(\tau^+ \rightarrow 3\pi \nu_\tau)$	$(9.31 \pm 0.05) \times 10^{-2}$	From PDG
$N(B_c^+ \rightarrow \tau^+ \nu_\tau)$	4295 ± 146	Uses $N_{b\bar{b}}$, f_c , \mathcal{B} 's, and ϵ
$N(B_c^+ \rightarrow J/\psi \mu^+ \nu_\mu)$	48670 ± 220	Uses $N_{b\bar{b}}$, f_c , \mathcal{B} 's, and ϵ
$\mathcal{B}(B_c^+ \rightarrow J/\psi \mu^+ \nu_\mu)$	0.0135 ± 0.0011	Calculation from O. Sumensari

17

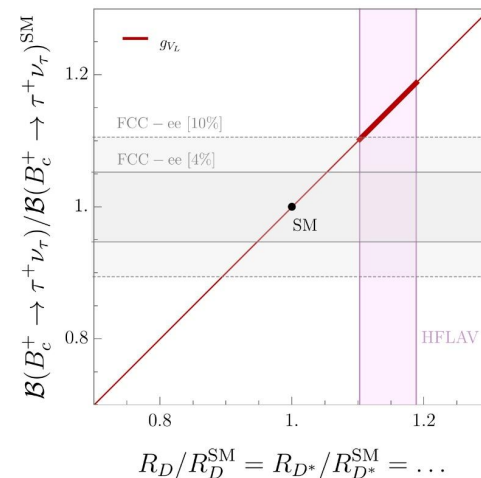
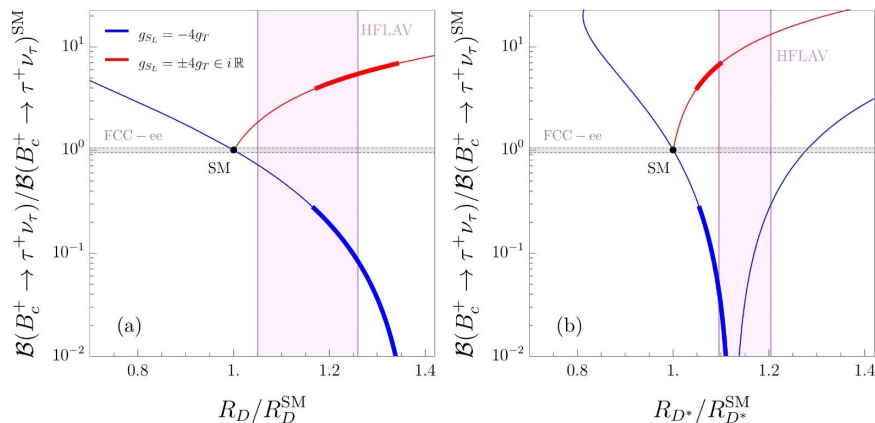
Anticipated precision on $B(B_c \rightarrow \tau \nu_\tau)$

$$B(B_c \rightarrow \tau \nu_\tau) = (1.941 \pm 0.175) \times 10^{-2}$$

- Recover the input branching ratio central value as expected
- Relative uncertainty is 9%, including uncertainties on all of the input terms
- Uncertainty dominated by the current theory uncertainty on $B(B_c \rightarrow J/\psi \mu \nu)$ 8.1%
 - Using [this](#) and [this](#) lattice paper for the current estimate along with exclusive $|V_{cb}|$
 - Uncertainty is reducible if decay form factors are measured e.g. in an angular analysis (LHCb and FCC-ee can both do this)
- Signal yield uncertainty from fit is 2.4%, which increases to 3.4% assuming the same level of systematics than statistics
 - Excellent precision using only one tau decay mode!

Sensitivity to New Physics

- Can consider the ratio $R_c = \mathcal{B}(B_c \rightarrow \tau \nu_\tau) / \mathcal{B}(B_c \rightarrow J/\psi \mu \nu_\mu)$ which has 4% precision
 - $|V_{cb}|$ independent, can assume no NP in the muonic mode for theory calculation
- R_c measurement at FCC-ee can strongly constraint both 2HDM and leptoquark parameter space in a complementary manner to other key observables
 - Leptoquark couplings can introduce O(10-100) variations



Summary



- FCC-ee offers a unique opportunity for flavour physics
 - Improve and complement measurements at LHCb upgrade and Belle II
- Full framework in place using common FCC SW tools
 - Event generation, processing, analysis
 - Many other exciting flavour modes need to be studied with the tools in place
- Selection exploiting missing energy signature of signal and 3π properties
 - Possible to achieve high purity final dataset
 - Analysis still feasible with higher background level (fit stable with 10 times large BG)
 - Signal yield measurement $\sim 3\%$ precision, but requires accurate $B(B_c \rightarrow J/\psi \mu \nu_\mu)$ prediction
 - R_c ratio also very valuable where 4% precision is achievable
- Preprint [arxiv:2105.13330](https://arxiv.org/abs/2105.13330) submitted to JHEP

Backup material



First stage MVA variables

The BDT is trained using the following features:

- Total reconstructed energy in each hemisphere;
- Total charged and neutral reconstructed energies in each hemisphere;
- Charged and neutral particle multiplicities in each hemisphere;
- Number of tracks in the reconstructed PV;
- Number of reconstructed 3π candidates in the event;
- Number of reconstructed vertices in each hemisphere;
- Minimum, maximum, and average radial distance of all decay vertices from the PV.

First stage MVA

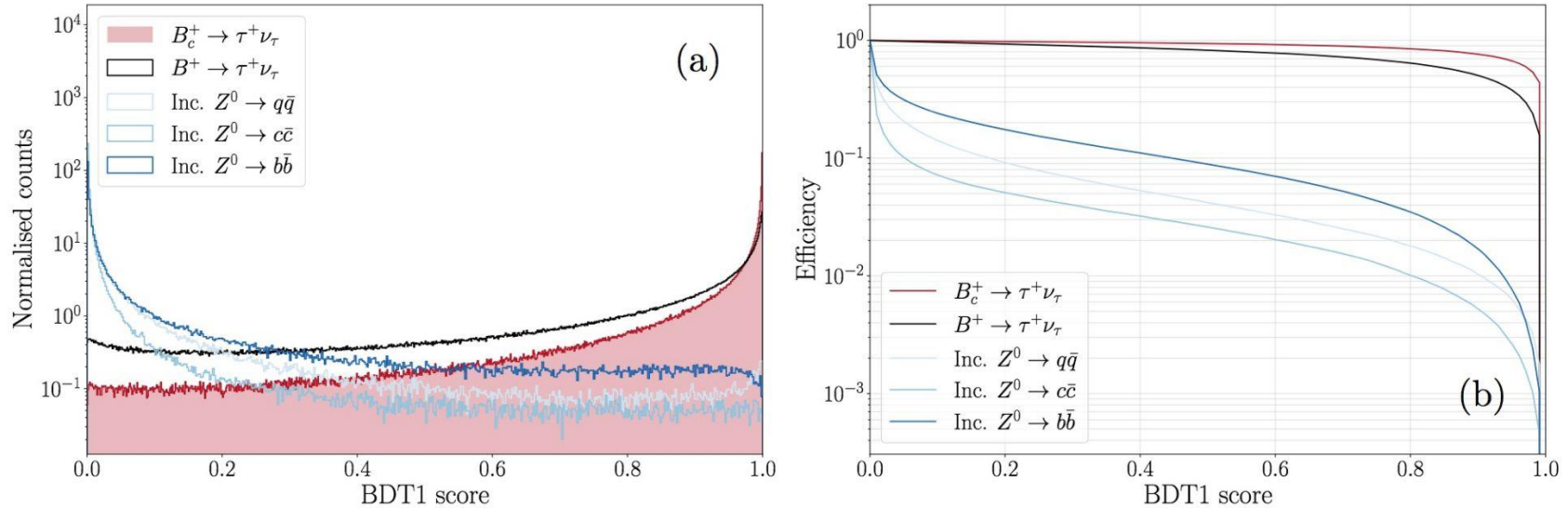


Figure 2: (a) First-stage BDT distribution in signal, $B^+ \rightarrow \tau^+ \nu_\tau$ background, and inclusive Z background. (b) Efficiency of the first-stage BDT as a function of cut value.

Second stage MVA variables

The BDT is trained on the following features:

- 3π candidate mass, and masses of the two $\pi^+\pi^-$ combinations;
- Number of 3π candidates in the event;
- Radial distance of the 3π candidate from the PV;
- Vertex χ^2 of the 3π candidate;
- Momentum magnitude, momentum components, and impact parameter (transverse and longitudinal) of the 3π candidate;
- Angle between the 3π candidate and the thrust axis;
- Minimum, maximum, and average impact parameter (longitudinal and transverse) of all other reconstructed decay vertices in the event;
- Mass of the PV;
- Nominal B energy, defined as the Z mass minus all reconstructed energy apart from the 3π candidate.

Second stage MVA

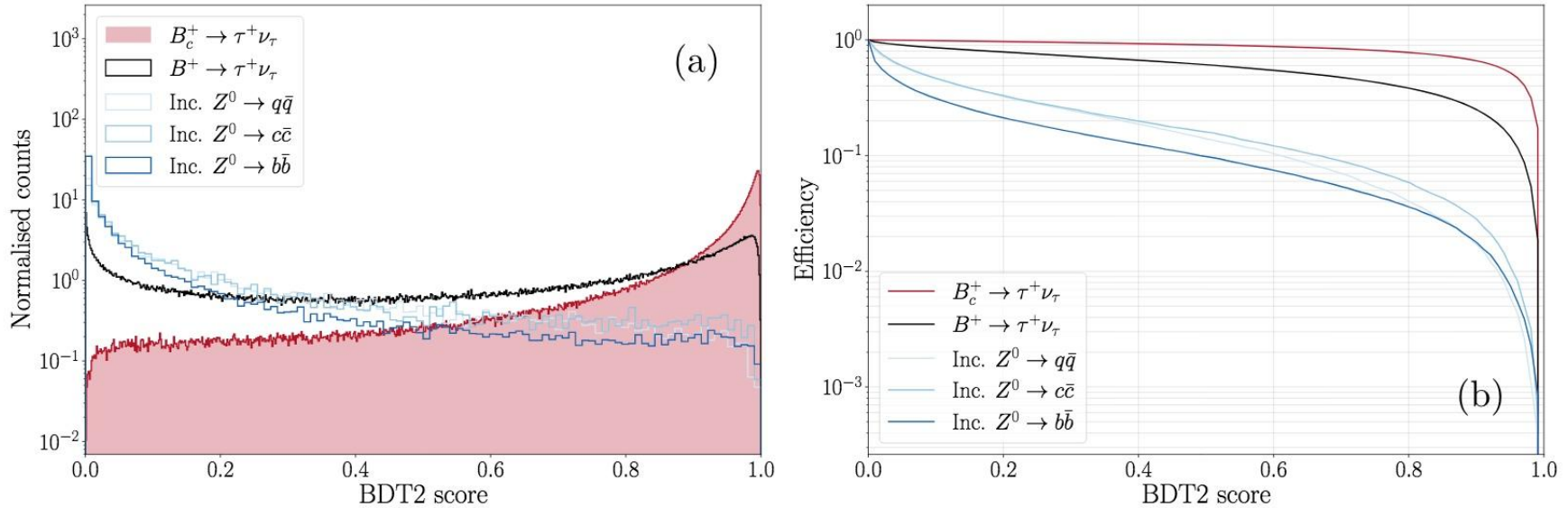


Figure 3: (Left) Second-stage BDT distribution in signal, $B^+ \rightarrow \tau^+ \nu_\tau$ background, and inclusive Z background. (Right) Efficiency of the second-stage BDT as a function of cut value.

Background composition

Prior to the BDT cut optimisation, none of the 10^9 inclusive $Z \rightarrow c\bar{c}$ and $Z \rightarrow q\bar{q}$ events are found to pass sufficiently tight cuts on both BDTs. As such, background from these sources is not considered in the optimisation or subsequent fit studies. After the same cuts, the remaining statistics in the inclusive $Z \rightarrow b\bar{b}$ sample are found to be insufficient for determining the background rejection accurately in the cut optimisation. To boost the background statistics for the optimisation, samples of exclusive b -hadron decays are generated, where the decay modes are chosen based on the composition of the remaining inclusive $Z \rightarrow b\bar{b}$ sample. The following decays are considered:

where $B \in \{B^0, B^+, B_s^0, \Lambda_b^0\}$ and the corresponding $D \in \{D^-, \bar{D}^0, D_s^-, \Lambda_c^-\}$. In each of the exclusive b -hadron samples, all of the b -hadron decay products are decayed inclusively. The list of exclusive decays considered is not exhaustive, and covers around 10% of the decay width for each B hadron. As a result, a factor 2.5 difference in rate relative to the inclusive $Z \rightarrow b\bar{b}$ sample is observed after tight BDT cuts. This factor is used to scale the exclusive sample yield estimates in the optimisation procedure, in order to avoid underestimating the expected background level.

- $B \rightarrow D\tau^+\nu_\tau$
- $B \rightarrow D^*\tau^+\nu_\tau$
- $B \rightarrow D\pi^+\pi^+\pi^-$
- $B \rightarrow D^*\pi^+\pi^+\pi^-$
- $B \rightarrow DD_s^+$
- $B \rightarrow D^*D_s^+$
- $B \rightarrow D^*D_s^{*+}$

Background estimation

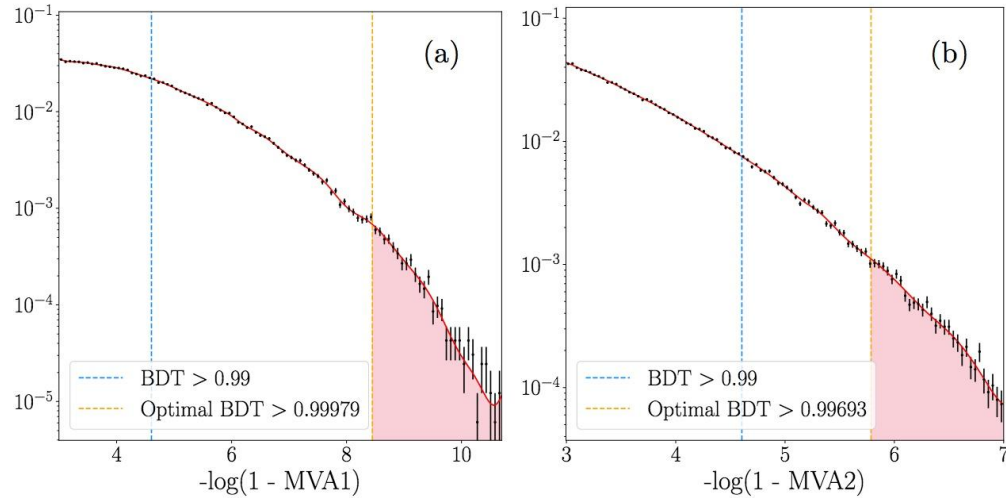


Figure 4: (a) BDT1 distribution above 0.95 for a combined sample of exclusive b -hadron decays. (b) BDT1 distribution above 0.95 for a combined sample of exclusive b -hadron decays. The cubic spline parameterisations are shown by solid red lines, example cuts of BDT > 0.99 by the dashed blue lines, and the optimal BDT cuts by the dashed orange lines. The background efficiency given prior cuts of > 0.95 on both BDTs is given by the product of the spline integrals above the optimal cuts (red areas), where each integral is normalised to the respective spline integral across the full range.

Discriminating variable

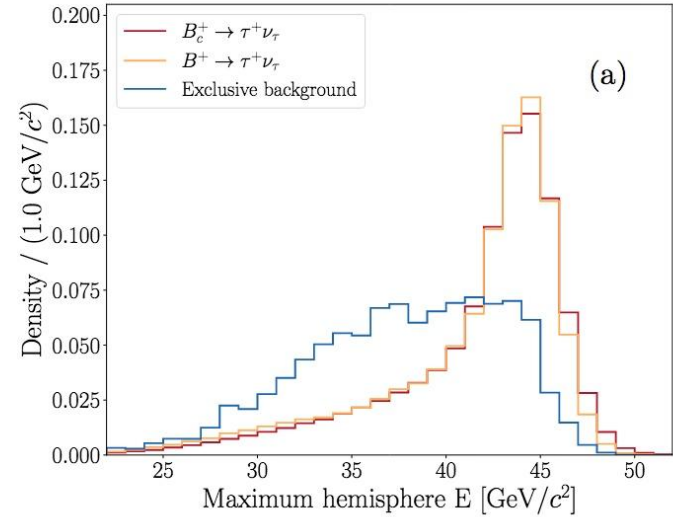
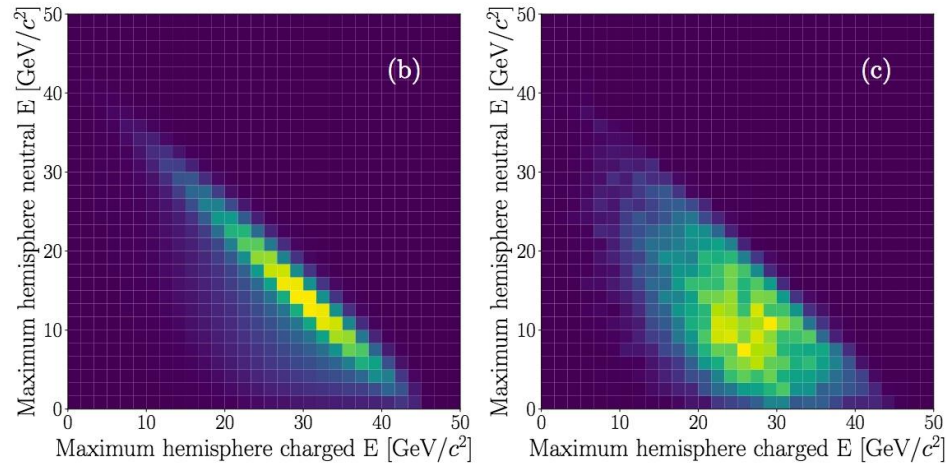


Figure 5: (a) Distribution of total hemisphere energy for the maximum energy hemisphere. Signal and $B^+ \rightarrow \tau^+ \nu_\tau$ decays closely follow the expected distribution for an inclusive b -quark decay from a Z , whereas the background distribution is biased downwards by the selection. (b/c) Relationship between the total charged and neutral energy in the maximum energy hemisphere for $B_c^+ \rightarrow \tau^+ \nu_\tau$ / inclusive $Z \rightarrow b\bar{b}$ events.

Fit

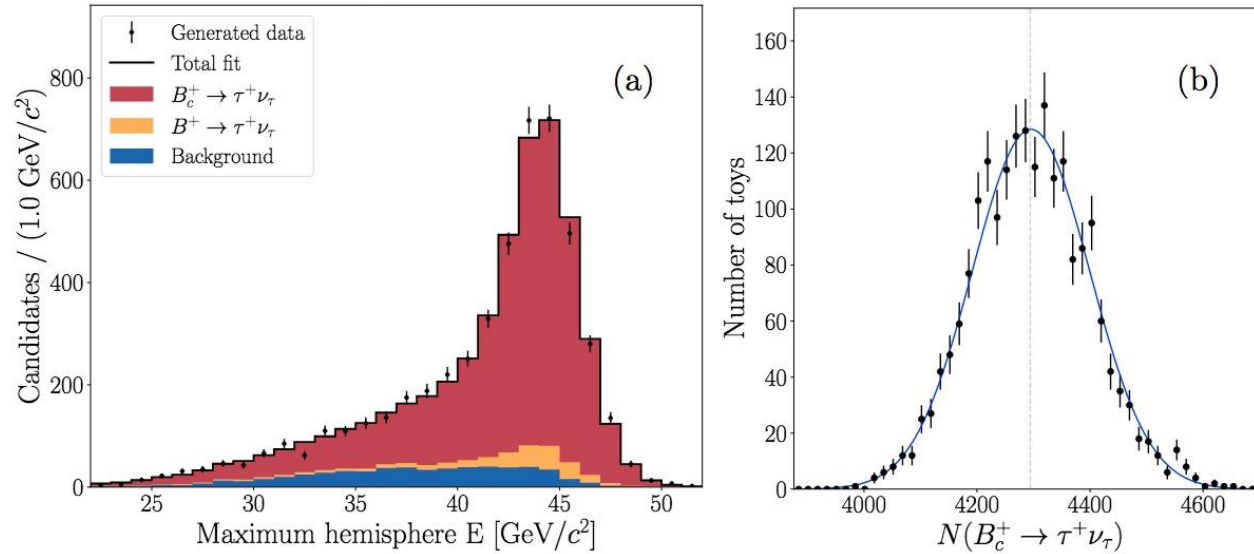


Figure 6: (a) Result of a single pseudoexperiment fit, where the peaking signal is clearly distinguishable from the background. (b) Signal yields measured in 2000 pseudoexperiment fits, where the generated value is indicated by the dashed vertical line.

Bc- \rightarrow Tau nu Yields

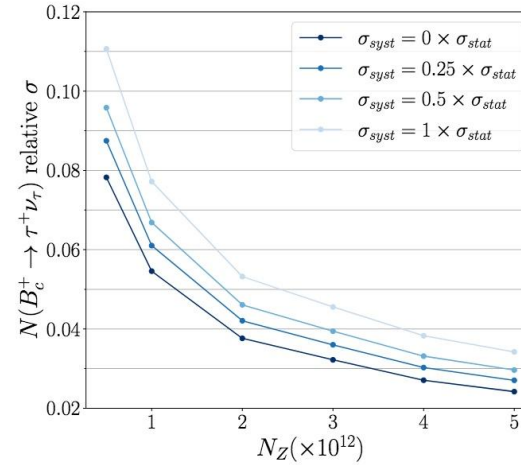


Figure 7: Relative precision on the signal yield as a function of N_Z . The signal yields at each N_Z value are taken from the cut optimisation procedure, and the statistical uncertainties are measured in pseudoexperiment fits. Different levels of systematic uncertainty relative to the statistical uncertainty are also shown.

$N_Z (\times 10^{12})$	$N(B_c^+ \rightarrow \tau^+ \nu_\tau)$	Relative σ (%)
0.5	430 \pm 33	7.8
1	858 \pm 46	5.5
2	1717 \pm 64	3.8
3	2578 \pm 83	3.2
4	3436 \pm 93	2.7
5	4295 \pm 103	2.4

Table 1: Estimated signal yields as a function of N_Z , where the uncertainties quoted are statistical only. The yield central values are determined from the cut optimisation procedure, and the uncertainties from pseudoexperiment fits.

Towards Branching Fraction

With $B_c^+ \rightarrow J/\psi\mu^+\nu_\mu$ as a normalisation mode, the ratio of branching fractions

$$\begin{aligned} R_c &= \frac{\mathcal{B}(B_c^+ \rightarrow \tau^+\nu_\tau)}{\mathcal{B}(B_c^+ \rightarrow J/\psi\mu^+\nu_\mu)} \\ &= \frac{N(B_c^+ \rightarrow \tau^+\nu_\tau)}{N(B_c^+ \rightarrow J/\psi\mu^+\nu_\mu)} \times \frac{\epsilon(B_c^+ \rightarrow J/\psi\mu^+\nu_\mu)}{\epsilon(B_c^+ \rightarrow \tau^+\nu_\tau)} \times \frac{\mathcal{B}(J/\psi \rightarrow \mu^+\mu^-)}{\mathcal{B}(\tau^+ \rightarrow \pi^+\pi^+\pi^-\bar{\nu}_\tau)} \end{aligned}$$

It is also possible to determine an absolute branching fraction for the signal decay,

$$\mathcal{B}(B_c^+ \rightarrow \tau^+\nu_\tau) = R_c \times \mathcal{B}(B_c^+ \rightarrow J/\psi\mu^+\nu_\mu)^{\text{SM}},$$

Results

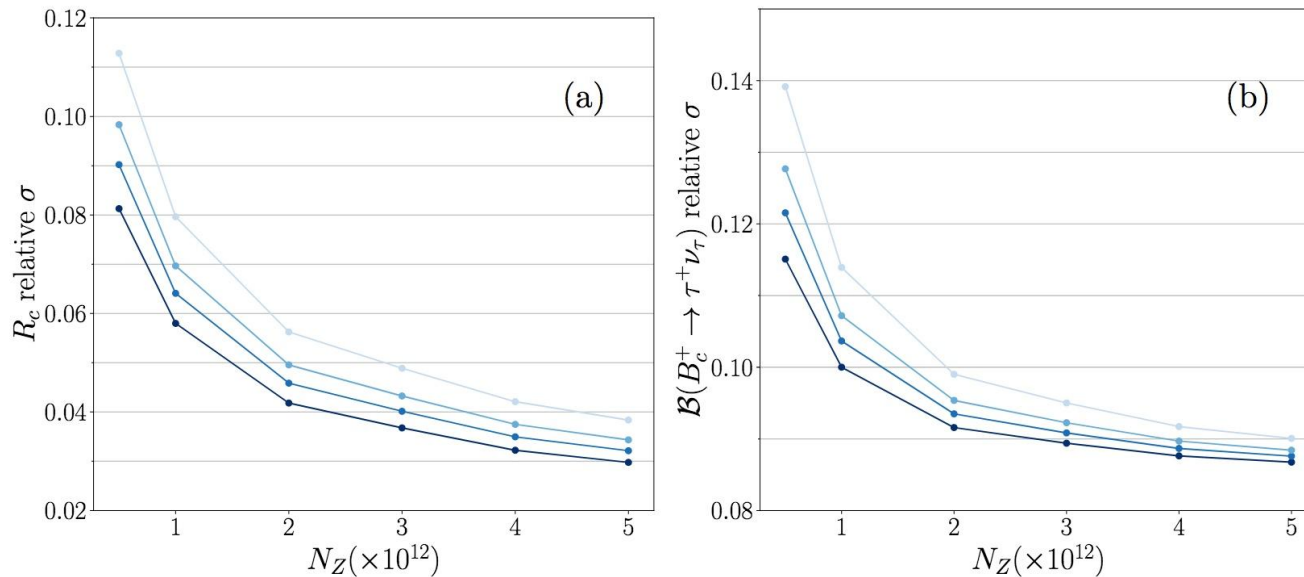


Figure 8: (a) Relative precision on the ratio of branching fractions $R = \mathcal{B}(B_c^+ \rightarrow \tau^+ \nu_\tau) / \mathcal{B}(B_c^+ \rightarrow J/\psi \mu^+ \nu_\mu)$ as a function of N_Z . (b) Relative precision on $\mathcal{B}(B_c^+ \rightarrow \tau^+ \nu_\tau)$ as a function of N_Z , using a SM prediction for $\mathcal{B}(B_c^+ \rightarrow J/\psi \mu^+ \nu_\mu)$. The different shades of blue correspond to different levels of systematic uncertainty on $N(B_c^+ \rightarrow \tau^+ \nu_\tau)$ relative to the statistical uncertainty, following the same colour scheme as Fig. 7.

New physics - 2HDM

Thanks to Olcyr Sumensari for the interpretation work, which is based on the analysis precision estimates

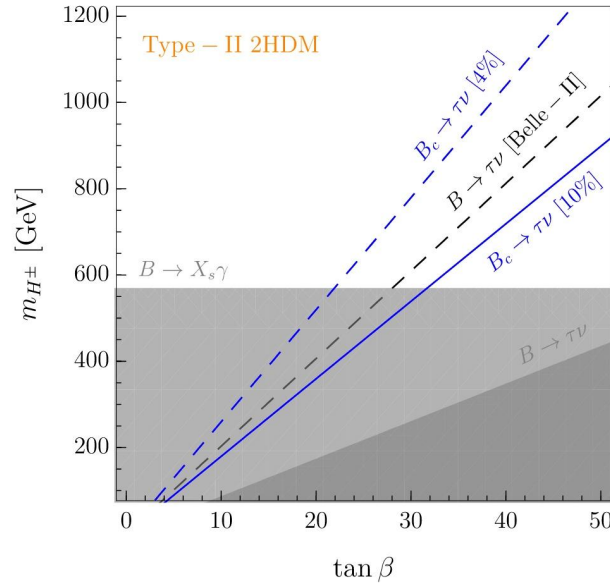


Figure 9: Expected constraints on the plane $\tan \beta$ vs. m_{H^\pm} for type-II 2HDM derived by assuming a relative uncertainty on $\Gamma(B_c^+ \rightarrow \tau^+ \nu_\tau)/|V_{cb}|^2$ of 10% (solid blue line) and 4% (dashed blue line). Current constraints obtained from $\mathcal{B}(B \rightarrow X_s \gamma)$ [64] and $\mathcal{B}(B^+ \rightarrow \tau^+ \nu_\tau)$ [61] are depicted by the grey regions. Prospects for a $\mathcal{B}(B^+ \rightarrow \tau^+ \nu_\tau)$ measurement at Belle-II are depicted by the grey dashed line, obtained under the assumption of 5% uncertainty on the branching fraction [69].

New physics - Leptoquarks

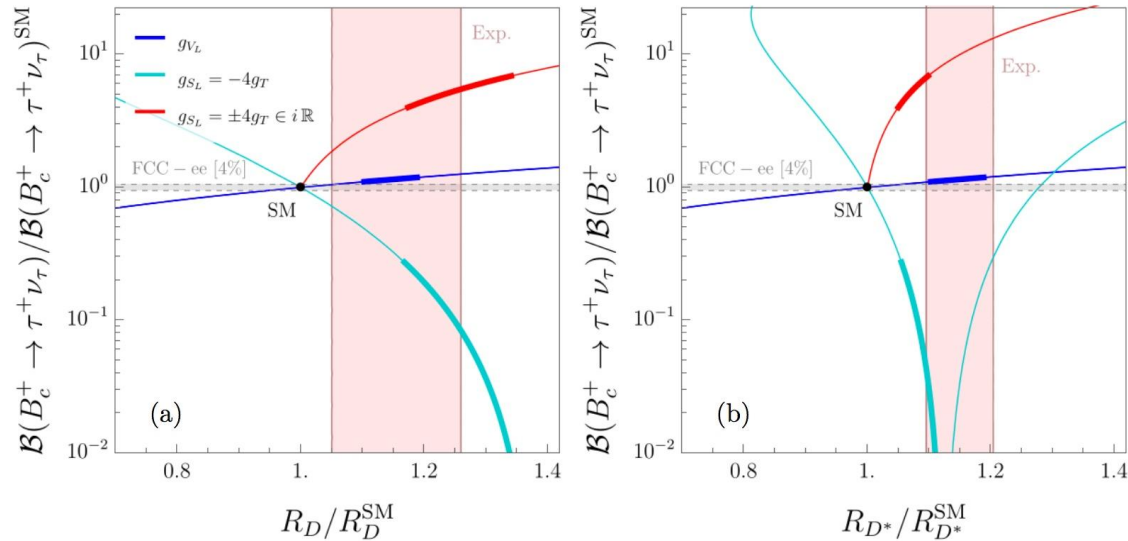


Figure 10: Predictions for (a) R_D/R_D^{SM} and (b) $R_{D^*}/R_{D^*}^{\text{SM}}$ are plotted against the ratio $\mathcal{B}(B_c^+ \rightarrow \tau^+ \nu_\tau) / \mathcal{B}(B_c^+ \rightarrow \tau^+ \nu_\tau)^{\text{SM}}$ in several effective scenarios: (i) g_{V_L} (blue), (ii) $g_{S_L} = -4g_T$ (cyan), and (iii) $g_{S_L} = +4g_T \in i\mathbb{R}$ (red), which are defined at $\Lambda \approx 1$ TeV. The thick lines correspond to the values of the effective couplings favoured by the current fit to $b \rightarrow c\tau\nu_\tau$ data [71]. The red shaded regions denote the current experimental averages of R_D and R_{D^*} at 1σ accuracy [23]. The grey region corresponds to the estimated sensitivity of 4% precision on $\Gamma(B_c^+ \tau^+ \nu_\tau) / |V_{cb}|^2$ at FCC-ee.

Summary

The sensitivities for both the branching fraction of $B_c^+ \rightarrow \tau^+ \nu_\tau$ and the ratio $R_c = \mathcal{B}(B_c^+ \rightarrow \tau^+ \nu_\tau) / \mathcal{B}(B_c^+ \rightarrow J/\psi \mu^+ \nu_\mu)$ are estimated as a function of the number of collected Z decays, where a relative precision of around 4% is achieved for R_c with $N_Z = 5 \times 10^{12}$. The precision on the absolute branching fraction is limited to around 8% due to knowledge of the $B_c^+ \rightarrow J/\psi \mu^+ \nu_\mu$ decay form factors, which can be improved through dedicated measurements of this mode in future.

The impact of a measurement of $B_c^+ \rightarrow \tau^+ \nu_\tau$ on NP scenarios is also discussed. In particular, it is shown that such a measurement at FCC-ee can constrain a large region of the $(\tan \beta, m_{H^\pm})$ plane in the type-II 2HDM, which cannot be covered by other flavour-physics measurements. Recently, leptoquark models have received significant attention as the only viable explanation of the B -physics anomalies in both charged and neutral current processes. A precise measurement of the branching fraction of $B_c^+ \rightarrow \tau^+ \nu_\tau$ at FCC-ee could fully probe the interpretations of R_D and R_{D^*} that are permitted under existing constraints.

In summary, this work demonstrates why FCC-ee is the most well-suited environment for a measurement of the branching fraction of the $B_c^+ \rightarrow \tau^+ \nu_\tau$ decay, and represents the first FCC-ee analysis to use common software tools from EDM4HEP through to final analysis.